

**P2X7 RECEPTOR ACTIVATES MULTIPLE SELECTIVE DYE PERMEATION
PATHWAYS IN RAW 264.7 AND HEK-293 CELLS***

Serife Cankurtaran-Sayar, Kemal Sayar, Mehmet Ugur

Department of Biophysics (SCS,MU) and Pharmacology and Clinical Pharmacology (KS)

Ankara University, School of Medicine, Siihiye, Ankara, TURKEY

Running Title: P2X7-Activated Selective Permeability

Corresponding Author: M. Ugur: Department of Biophysics, Ankara University

School of Medicine, Sıhhiye Ankara, TURKEY 06100.

Tel: + 90 312 3103010 / 337

E-mail: mugur@medicine.ankara.edu.tr

Number of text pages: 37

Number of tables: 1

Number of figures: 7

Number references: 21

Number of words in abstract: 242

Number of words in Introduction: 612

Number of words in Discussion: 1515

Abbreviations used : $[Ca^{2+}]_i$, Intracellular Ca^{2+} concentration; Fura-2 AM, Fura 2 acetoxymethyl ester; HEK, Human embryonic kidney; HEK-rP2X7, HEK-293 cells transfected with rat P2X7 receptors; DMEM, Dulbecco's modified Eagle's medium; RPMI, Roswell Park Memorial Institute; BAPTA, 1,2-bis(2-aminophenoxy) ethane N,N,-N',N'-tetraacetic acid; ICCD, Intensified charge coupled device; ROI, Region of interest.

ABSTRACT

P2X7 receptor has gained an increasing importance as a drug target. One important response to P2X7 receptor stimulation is the uptake of large molecular weight tracers into cells. However, mechanism for this response is not understood clearly, but it is generally believed that a non-selective large pore protein forms this P2X7 receptor activated permeability pathway. We examined human embryonic kidney-293 (HEK-293) cells transfected with rat P2X7 receptors (HEK-rP2X7) and a macrophage derived cell line RAW 264.7 that expresses an endogenous P2X7 receptor. We used confocal microscopy to investigate uptake of different types of dyes into these cells after ATP application. Stimulation of P2X7 receptors in HEK-rP2X7 cells activated two different dye uptake pathways; one that was permeable to cationic fluorescent dyes, YO-PRO-1 and TO-TO-1, but not to anionic dyes, lucifer yellow or calcein, and did not require intracellular Ca^{2+} concentration ($[\text{Ca}^{2+}]_i$) increase to be activated. The second pathway permeated only lucifer yellow and was completely dependent on $[\text{Ca}^{2+}]_i$ for activation. In RAW 264.7 cells P2X7 receptor stimulation activated uptake of ethidium, YO-PRO-1, TO-TO-1, lucifer yellow and calcein. Again two different permeation pathways were discerned in RAW 264.7 cells, one permeated only ethidium and the other one lucifer yellow. We did not observe any clear $[\text{Ca}^{2+}]_i$ dependence for these permeation pathways. Our results demonstrate that instead of a single non-selective pore, P2X7 receptor appears to activate at least two permeation pathways, one for cationic and one for anionic dyes with different activation properties.

INTRODUCTION

P2X7 receptor is a member of P2X receptor family comprised of ligand-gated ion channels. Activated P2X7 receptor causes not only a cationic membrane current, but also permeabilization of the cell membrane to large molecular weight molecules (North, 2002; Ralevic and Burnstock, 1998; Surprenant et al, 1996). This permeabilization response is usually observed and measured by using large fluorescent molecules as tracers, which normally can not cross the cell membrane.

P2X7 receptors are known to be important in the pathophysiology of arthritis and mediation of pain (See for a review Donnelly-Roberts and Jarvis 2007). In spite of the considerable interest on the role of P2X7 receptors in pathophysiological processes and also as a drug target in recent years, the physiological role of the permeabilisation response is currently not clear. For example, it has been shown that pannexin-1 knock-down inhibited both the P2X7 receptor-induced dye uptake and IL-1 β release but not the cationic current (Pelegriin and Surprenant, 2006), but the connection between dye uptake and IL-1 β release has not been well understood. More importantly, the precise character of the “large molecule-permeation pathway” that is activated by P2X7 receptor is also unclear, which greatly contributes to the uncertainty about its function. The generally accepted view in the literature is that the permeation pathway which mediates the P2X7 receptor-induced uptake is a non-selective pathway, such as a large pore, which basically permeates all molecules smaller than 900-1000 Da. (North, 2002; Schilling et al, 1999; Steinberg et al, 1987). Results obtained by using the cell-attached mode of patch clamp technique has also been published indicating that pores with large electrical conductivity may mediate the P2X7 receptor-induced dye uptake responses (Coutinho-Silva and Persechini, 1997; Faria et al, 2005; Faria et al, 2009). Initially,

P2X7 receptor itself was thought to dilate and become permeable to these large molecules (Khakh et al 1999). However growing evidence suggests that a pathway distinct from the P2X7 receptor actually mediates the permeation of large tracer molecules (Faria et al, 2005; Schilling et al, 1999; Yan et. al 2008). Recently, this P2X7 receptor-activated dye permeation pathway was proposed to be formed by a gap-junction protein, pannexin-1, which is also known to form functional “hemichannels” (North, 2002; Pelegrin and Surprenant, 2006; Pelegrin and Surprenant, 2007). Current knowledge about the permeation properties of this hemichannel somewhat complies with the current non-selective pore model of the P2X7 receptor-activated permeation pathway (Bao et al, 2004; Locovei et al, 2006, Locovei et al, 2007).

Published reports seem to support a non-selective permeation pathway (which may or may not be a pore) hypothesis. Different studies have shown that, various types of cells can uptake molecules with different chemical structures and molecular weights (such as negatively charged dye lucifer yellow and positively charged dyes YO-PRO-1 and ethidium) after P2X7 receptor stimulation. (Le Stunff and Raymond, 2007; Pelegrin and Surprenant, 2006; Schilling et al, 1999; Steinberg et al, 1987; Surprenant et al, 1996; Yan et al, 2008; Faria et al, 2009). However, a recent study presented evidence that the uptake pathways activated by P2X7 receptor may be selective (Schachter et al, 2008).

The contradictory data about the dye selectivity of the P2X7 receptor activated permeation pathway prompted us to investigate whether the P2X7 receptor-activated dye permeability pathway behaves like a non-selective pore or not. Using fluorescent tracers with different sizes and charges we systematically studied the permeation properties of P2X7 receptor-activated dye permeability in RAW 264.7 cells that endogenously express P2X7 receptor and a human embryonic kidney -293 (HEK-293)

cell clone that is transfected with the same receptor (HEK-rP2X7). Our results indicate that in these cells P2X7 receptor-activated dye uptake is mediated by several selective pathways, rather than a single non-selective one.

MATERIALS AND METHODS

Chemicals and solutions. BAPTA-AM, fura2-AM, YO-PRO-1, TO-TO-1 and Geneticin were from Invitrogen (Karlsruhe, Germany), lucifer yellow and calcein were from SIGMA (Taufkirchen, Germany), ethidium bromide was from Fischer Scientific (New Jersey, USA) and EGTA was from Acros Organics (New Jersey, USA). Cell culture media, fetal calf serum and antibiotics were from Biological Industries (Kibbutz Bete Haemek, Israel). All other chemicals were from SIGMA (Taufkirchen, Germany) and Fischer Scientific (New Jersey, USA).

We used a nominally divalent-free KCl bathing solution containing; K^+ 150, Na^+ 5, HEPES 10 mM, pH 7.8 (w / KOH) with no added divalent cations or a nominally divalent-free NaCl bathing solution containing; Na^+ 150, K^+ 5, Hepes 10 mM, pH 7.4 (w / NaOH) with no added Ca^{2+} . In some experiments 1, 1.2 or 5 mM Ca^{2+} was added to these bathing solutions. In some experiments, cells were incubated in the presence of BAPTA-AM (20 μ M) in nominally Ca^{2+} free bathing solution for 50 minutes in room temperature to prevent ATP-induced intracellular Ca^{2+} concentration ($[Ca^{2+}]_i$) increase.

Cell Culture and Transfection. HEK-293 cells were transfected with the rat P2X7 receptor c-DNA (A kind gift from Dr. Alan North) by using lipofectamin. Stable clones were selected using Geneticin (700 μ g/ml). Geneticin-resistant clones were further selected according to the strength of their $[Ca^{2+}]_i$ increase and YO-PRO-1 uptake responses following extracellular ATP (1 mM) application. The stable clone thus selected will be referred to as HEK-rP2X7 cells in the text. HEK-rP2X7 cells and RAW 264.7 cells were grown in DMEM (Dulbecco's modified Eagle's medium) and RPMI-1640 (Roswell Park Memorial Institute) media respectively, both supplemented with penicillin (100 IU/ml), streptomycin (100 μ g/ml) and 10% (v/v) fetal calf serum, at 37°C in a humidified atmosphere of 5% CO₂.

Measurement of DNA-Binding Fluorescent Dye Uptake. RAW 264.7 and HEK-rP2X7 cells were grown to 70-80% confluency on glass cover-slips. These cover-slips were then placed in a bathing chamber mounted on a heated microscope stage. Cells were first incubated for 5-10 min. with the DNA-binding fluorescent dyes, ethidium bromide, YO-PRO-1, or TO-TO-1 which were added to the bathing solution at 10, 5 and 5 μ M final concentrations respectively. ATP was then applied at a final concentration of 1 mM. The fluorescence increase due to the binding of these dyes to cell DNA was recorded as a measure of cell permeability increase. This fluorescence change was measured by using either a confocal microscope (Leica TCS-SP5 DMI 6000, Leica Microsystems GmbH, Mannheim, Germany) or alternatively an intensified charge coupled device (ICCD) camera and a microscope based spectrofluorimetry system (TE-200, Nikon, Japan and Delta-Ram illuminator IC-300 ICCD camera, Photon Technologies International, New Jersey, USA). Laser line at 488 or 514 nm from the argon laser was utilized for dye excitation. Data were collected by using Leica Advance Fluorescence (Leica Microsystems GmbH, Mannheim, Germany) or Image-master (Photon Technologies International, New Jersey, USA) soft wares. As both the RAW 264.7 and the HEK-rP2X7 cells went through an extensive change of shape and detach from the cover slip and move along z-axis after ATP stimulation, we collected a set of z-stacks for every time point to be able to track the cells as they move away from the cover slip during confocal microscope measurements. We used a large pinhole to obtain a large depth of field and maximum light gathering ability. We integrated the fluorescence coming from all the z-planes (thickness of the z-stacks was between 20-40 μ m depending on the type of application, with 2 μ m steps) and then calculated the total fluorescence intensity coming from a volume rather than a plane. For the HEK-rP2X7 cells, we used the total signal of a cell population within a field of view, as tracking of

individual cells was extremely difficult. For the RAW 264.7 cells, on the other hand, tracking of individual cells was possible. So the fluorescence was measured from individual cells using a region of interest (ROI) enclosing the whole cell. All measurements were performed at 37 ° C.

In HEK-rP2X7 cells, as changes in the number of cells within the field of view could affect the rate of fluorescence increase, YO-PRO-1 uptake experiments were also carried out with suspended cells using a cuvette spectrofluorimeter (JASCO FP-6500, Japan) with constant stirring at 37 ° C. For quantitative comparisons this method was preferred because the observed fluorescence values could be normalized according to a maximum obtained by Triton X-100 permeabilization. For cuvette experiments, HEK-rP2X7 cells were first detached by using EDTA-PBS and kept at 37° C in a 5% CO₂ incubator for 45-60 minutes to recover.

Measurement of Negatively Charged Fluorescence Dye Uptake. Unlike the positively charged dyes which become fluorescent only after binding to DNA, negatively charged dyes Lucifer yellow and calcein give spontaneous fluorescence. Hence, in the bathing solution containing these dyes, cells first appear as dark areas on a bright fluorescent background in optical slices obtained by the confocal microscope,. As cells start to uptake these dyes an increase in the fluorescence of the intracellular region occurs. This intracellular fluorescence increase can easily be discriminated from the extra-cellular fluorescence, and measured as a function of time.

For these experiments, cells were grown and handled as described above. Lucifer yellow or calcein were used at a final concentration of 500 µM. Because the cells detached from the cover slips and moved along z-axis, we gathered a series of z-sections for each time point similar to what is described above. Data was collected and analyzed by using Leica Advance Fluorescence software (Leica Microsystems GmbH,

Mannheim, Germany). Intracellular fluorescence was measured as an average value from a ROI within the cell and given as the ratio of intracellular signal over the signal from a ROI, right outside the cell. For each cell, fluorescence was measured from the most suitable z-section. A small pinhole value (1 Airy unit) for optimum z-resolution was used. Dyes were excited either by 458 or 488 nm line of the Argon laser depending on the type of the dye. All measurements were performed at 37° C.

When lucifer yellow and ethidium fluorescence was measured simultaneously in RAW 264.7 cells, sequential illumination and detection mode of the confocal microscope was used to minimize dye interference, observed bleed-through between dyes was small.

Measurement of Intracellular Ca^{2+} Concentration. Cells were incubated with fura-2 AM (4 μ M) for 50 minutes at room temperature and washed. Following a 15 minute period, ATP (1 mM) was applied and $[Ca^{2+}]_i$ change was measured by using a PMT and a microscope based spectrofluorimetry system (TE-200, Nikon, Japan and PTI-ratiomaster system, Photon Technologies International, New Jersey, USA) or a cuvette spectrofluorimeter (FP-6500, JASCO, Japan). Fluorescent emissions with 340, 360, 380 nm excitation were measured at 510 nm. All $[Ca^{2+}]_i$ measurements were performed at 37 °C.

LDH Release Measurements. Lactate dehydrogenase enzyme (LDH) released from cells was measured after application of ATP (1 mM) in nominally Ca^{2+} free bathing solutions in HEK-rP2X7 and RAW 264.7 cells, by using Roche Cytotoxicity Detection Kit (Roche Diagnostics GmbH, Mannheim, Germany) according to the manufacturer's instructions. LDH values were normalized according to total cell LDH.

Data analysis and statistics. In this study as we mainly interested in either the presence or the absence of a very clearly identifiable response, rather than its magnitude, we give statistical data in order to give an idea about the strength of the

responses in general. The responses were highly repeatable. We used students-t test for comparison of the mean values when quantitative assessment was necessary and considered the difference not significant for p values larger than 0.05.

RESULTS

We used HEK-293 cells stably expressing rat P2X7 receptors and RAW 264.7 cells to investigate P2X7 receptor-activated uptake of several fluorescent probes. Uptake of positively charged dyes such as YO-PRO-1 was assessed by using a confocal microscope, but an ICCD camera-attached fluorescent microscope or a cuvette spectrofluorimeter were also employed to confirm confocal data. Uptake of negatively charged dyes such as lucifer yellow was assessed in thin confocal optic-slices. In most of our experiments, we used a high K^+ bathing solution for two reasons: i) to avoid intracellular K^+ depletion which may effect the dye uptake (Pelegrin and Surprenant, 2007) and increase cell death after P2X7 receptor activation, and ii) to minimize the complicating effect of membrane potential change that may occur after P2X7 receptor-mediated cationic current activation. Nevertheless, we repeated all the key experiments in a NaCl bathing solution for comparison in both RAW 264.7 and HEK-rP2X7 cells and obtained essentially similar results (Data not shown).

Similar to earlier reports, we observed that extracellular application of high dose of ATP (1 mM) permeabilized HEK-rP2X7 and also RAW 264.7 (a macrophage derived cell-line) cells to large molecular weight fluorescent dyes such as YO-PRO-1 (Le Stunff and Raymond, 2007; Pelegrin and Surprenant, 2007; Steinberg et al, 1987; Surprenant et al, 1996). This permeabilization was accompanied by an extensive blebbing in both cell types (Fig. 1, Supplement-Fig. 1), which was followed by detachment of the cells from the cover slip. This shape change was more marked in HEK-rP2X7 cells than in RAW 264.7 cells.

ATP-Induced Dye Uptake into HEK-rP2X7 and RAW 264.7 Cells is Due to P2X7 Receptor Activation. Two lines of evidence suggest that the observed ATP-induced increase in fluorescent dye permeability and blebbing are due to P2X7 receptor

activation in both cell types: i) Untransfected HEK-293 cells which do not express P2X7 receptors did not show any YO-PRO-1 or lucifer yellow permeability or blebbing after ATP (1 mM) stimulation. (Data not shown) ii) 2', 3'-O-(benzoyl-4-benzoyl)-ATP (BzATP), an agonist with higher efficacy and potency compared to ATP at P2X7 receptors, permeabilized RAW 264.7 cells to YO-PRO-1 when used at a concentration of 20 μ M whereas the same concentration of ATP was completely ineffective in inducing YO-PRO-1 uptake in the same cells. Additionally, UTP (1 mM), an agonist for P2Y but not P2X7 receptors, did not induce any YO-PRO-1 or lucifer yellow uptake in RAW 264.7 cells (Data not shown). These results in RAW 264.7 cells are consistent with an agonist profile for P2X7 receptor.

HEK-rP2X7 Cells can Uptake Both YO-PRO-1 and Lucifer Yellow after ATP

Stimulation in the Presence of Extracellular Ca²⁺. In HEK-rP2X7 cells, in agreement with previous studies (Surprenant et al, 1996; Virginio et al, 1999), ATP (1 mM) applied in a Ca²⁺ (1 mM)-containing bathing solution induced a strong YO-PRO-1 uptake response (Fig. 2A), (Ratios of fluorescence measured 15 minutes after vehicle or ATP application over the initial value were 1.35 ± 0.17 and 76.99 ± 18.90 , respectively. $p < 0.01$). YO-PRO-1 is a cationic DNA-binding dye with a molecular weight of 375 Da. ATP stimulation also triggered uptake of a much larger cationic dye, TO-TO-1 (MW: 894 Da, Supplement-Fig. 2). In the same Ca²⁺-containing bathing solution, ATP stimulation (1 mM) also resulted in a clear uptake of the anionic dye, lucifer yellow (MW: 433 Da; Fig. 2B) into HEK-r2X7 cells. In the absence of ATP stimulation, basal uptake of all these dyes was negligible. Both YO-PRO-1 and lucifer yellow uptake responses were very repeatable, they were observed in all of the coverslips we used in Ca²⁺-containing solutions.

ATP-Induced Uptake of Lucifer Yellow but not of YO-PRO-1 into HEK-rP2X7 Cells Requires the Presence of Extracellular Ca²⁺. When ATP (1 mM) was applied to HEK-rP2X7 cells in the nominally Ca²⁺-free bathing solution, we observed, to our surprise, that uptake of the anionic dye lucifer yellow that was so clear in Ca²⁺-containing bathing solution, disappeared completely (Fig. 2B). (Ratios of intracellular fluorescence measured 15 minutes after ATP application over the initial value were 0.94 ± 0.06 and 4.70 ± 1.39 in the absence and presence of extracellular Ca²⁺ respectively, $p < 0.05$). In contrast, ATP-induced uptake of cationic dye YO-PRO-1 (Fig. 2A) was slightly increased but not manifestly affected by the removal of Ca²⁺ from the bathing solution. (YO-PRO-1 fluorescence measured 15 minutes after ATP application in the absence of Ca²⁺ was $125\% \pm 16$ of that measured in the presence of Ca²⁺). This observation for YO-PRO-1 is in agreement with what was previously reported (Virginio et al, 1997).

We also measured YO-PRO-1 uptake from larger populations of cells using a cuvette-based assay to compare (in a more precise way) the kinetics of YO-PRO-1 dye uptake in the presence and absence of extracellular Ca²⁺. In these experiments, we found that extracellular Ca²⁺ did not have any prominent effect on YO-PRO-1 uptake (Fig 3A) strengthening the confocal microscope measurements (Compare Fig 2A and 3A). Removal of Ca²⁺ from the bathing solution slightly raised the time constant of the single exponential function fitted to the time course of YO-PRO-1 fluorescence increase, but did not otherwise seriously affect it (The maximum fluorescence increase values obtained in the presence and absence of Ca²⁺ were $37 \pm 4\%$ and $43 \pm 5\%$ of the maximum fluorescence obtained by Triton X-100, respectively. Time constants were $1.00 \cdot 10^{-3} \pm 0.06 \cdot 10^{-3}$ and $1.49 \cdot 10^{-3} \pm 0.18 \cdot 10^{-3} \text{ s}^{-1}$, in the presence and absence of Ca²⁺, respectively. For time constants $p < 0.05$).

Another anionic dye, calcein (MW: 623 Da), on the other hand, did not enter into HEK-rP2X7 cells in response to ATP stimulation either in the presence or in the absence of extracellular Ca^{2+} in any of the 3 experiments performed on 3 different days (Fig. 2C). A summary of the ATP-induced dye uptake results in HEK-rP2X7 cells can be seen in Table 1.

Intracellular $[\text{Ca}^{2+}]$ Increase Induces a Lucifer Yellow but not of YO-PRO-1 Uptake in to HEK-rP2X7 Cells in the Absence of ATP Stimulation. Strict dependence of the ATP-stimulated lucifer yellow uptake on the presence of extracellular Ca^{2+} but the apparent independence of the YO-PRO-1 uptake from Ca^{2+} prompted us to investigate whether the lucifer yellow uptake response can selectively be induced by $[\text{Ca}^{2+}]_i$ increase without P2X7 receptor stimulation. In HEK-rP2X7 cells, increasing $[\text{Ca}^{2+}]_i$ by Br-A23187 application induced uptake of lucifer yellow (Ratios of intracellular fluorescence measured 20 minutes after ionophore application over the initial value were 1.18 ± 0.02 and 4.89 ± 0.91 in the absence and presence of Br-A23187 respectively, $p < 0.01$) but not of YO-PRO-1 (Ratios of intracellular fluorescence measured 20 minutes after ionophore application over the initial value were 1.16 ± 0.04 and 1.09 ± 0.06 in the absence and presence of Br-A23187 respectively) or calcein (Supplement Fig. 3). This result further suggests that lucifer yellow and YO-PRO-1 are taken in to HEK-rP2X7 cells by two different pathways, one of them is Ca^{2+} -activated and the other one is not.

Intracellular $[\text{Ca}^{2+}]$ Increase is not a Prerequisite for ATP-Induced YO-PRO-1 Uptake into HEK-rP2X7 Cells. We further investigated the role of $[\text{Ca}^{2+}]_i$ in ATP-induced YO-PRO-1 uptake by incubating HEK-rP2X7 cells with BAPTA-AM (20 μM for 60 minutes) and applying ATP (1 mM) in EGTA (1 mM) containing Ca^{2+} -free bathing solution. With confocal microscope, in attached cells, we did not observe any

inhibitory effect of BAPTA loading on the responses to ATP applied in EGTA containing bathing solutions (Data not shown). However, as discussed in materials and methods section, the detachment of HEK cells became severe in EGTA-containing bathing solution and hampered a precise quantitative assessment of YO-PRO-1 uptake kinetics. Hence, we repeated these experiments in suspended cells using a cuvette spectrofluorimeter. Even under these stringent Ca^{2+} -buffering conditions ATP-induced YO-PRO-1 uptake, albeit slowed down to some extent, was not abolished (Fig. 3B). The maximum fluorescence values were $50 \pm 5 \%$ and $43 \pm 3 \%$ of the maximum fluorescence obtained by Triton X-100 and the time constants were $0.85 \cdot 10^{-3} \pm 0.07 \cdot 10^{-3}$ and $1.64 \cdot 10^{-3} \pm 0.06 \cdot 10^{-3} \text{ s}^{-1}$, in the presence and absence of Ca^{2+} buffers, respectively. For time constants $p < 0.001$). This result shows that an elevation of $[\text{Ca}^{2+}]_i$ is not essential for activation of P2X7 receptor-mediated YO-PRO-1 uptake into HEK-rP2X7 cells.

We made $[\text{Ca}^{2+}]_i$ measurements in fura-2-loaded, suspended HEK-rP2X7 cells to control the effectiveness of our Ca^{2+} buffering strategy. We observed no measurable $[\text{Ca}^{2+}]_i$ change with ATP stimulation in any of the experiments we performed under these buffered conditions whereas a clear and sustained ATP-induced $[\text{Ca}^{2+}]_i$ increase was observable in the nominally Ca^{2+} -free bathing solutions in the absence of buffers (Fig. 3B inset). These results indicate that the buffers we used can effectively prevent the $[\text{Ca}^{2+}]_i$ increase induced by ATP application in HEK-rP2X7 cells. We obtained essentially the same results in attached cells (Data not shown).

Given the fact that P2X7 receptor stimulation can increase $[\text{Ca}^{2+}]_i$ in nominally Ca^{2+} -free bathing solution, why lucifer yellow uptake into HEK-rP2X7 cells can only be stimulated by ATP in Ca^{2+} -containing solution, but not in Ca^{2+} -free solution, is not immediately clear. To clarify this point we measured $[\text{Ca}^{2+}]_i$ increase induced by P2X7

receptor stimulation in the presence and absence of extracellular Ca^{2+} , but without any Ca^{2+} -buffering, in attached cells. We found that ATP-induced $[\text{Ca}^{2+}]_i$ increase was substantially smaller in the nominally Ca^{2+} -free bathing solution than in Ca^{2+} (1 mM) containing solution (Supplement-Fig 4). Average fura-2 fluorescence ratios 10 minutes after ATP application were 2.91 ± 0.37 and 1.09 ± 0.19 in the presence and absence of extracellular Ca^{2+} , respectively. $p < 0.05$). This result suggests that the maximum level of $[\text{Ca}^{2+}]_i$ reached after P2X7 receptor stimulation is critical in lucifer yellow uptake response. (The $[\text{Ca}^{2+}]_i$ increase in nominally Ca^{2+} -free bathing solution is probably due to contaminating Ca^{2+} in the bathing solution as it can significantly be reduced only by addition of EGTA).

RAW 264.7 Cells can Uptake Positively as well as Negatively Charged Dyes After ATP Stimulation in Nominally Ca^{2+} -free Bathing Solution. Confocal microscope (and also ICCD camera) measurements showed that upon stimulation with ATP (1 mM) in nominally Ca^{2+} -free bathing solutions, RAW 264.7 cells could uptake positively charged DNA-binding dyes ethidium, YO-PRO-1, TO-TO-1 and also the anionic dyes lucifer yellow and calcein (Fig. 4A & 4B and Supplement-Figs. 5A-E). All these dyes had a substantially slower uptake into RAW 264.7 cells in the absence of ATP (Supplement-Figs. 5A-E) (Ratios of YO-PRO-1 fluorescence measured 15 minutes after vehicle or ATP application over their initial values were 1.05 ± 0.07 and 4.26 ± 0.70 , respectively, $p < 0.01$. The same values were 1.27 ± 0.12 and 8.31 ± 1.52 for lucifer yellow. $p < 0.01$). These findings indicate that ATP stimulation in a Ca^{2+} -free bathing solution can render RAW 264.7 cells permeable to a range of positively and negatively charged dyes with very different molecular weights.

Extracellular Ca^{2+} does not Affect the Uptake of YO-PRO-1 into RAW 264.7 Cells but Blocks ATP-Induced Uptake of Lucifer Yellow. In confocal microscope measurements,

we did not observe any measurable inhibitory effect of extracellular Ca^{2+} on the ATP-induced YO-PRO-1 uptake into RAW 264.7 cells in any of the 5 experiments we performed as pairs on different days (Average YO-PRO-1 uptake measured 10 minutes after ATP application in the Ca^{2+} -containing bathing solution was 114 ± 7 of that in Ca^{2+} free solution) (Fig. 4A.). Interestingly and in contrast to these findings, when ATP (1 mM) was applied to RAW 264.7 cells in a Ca^{2+} (1 mM)-containing bathing solution, kinetics of lucifer yellow uptake significantly slowed down in all of the 4 experiments performed as pairs: Lucifer yellow uptake measured 10 minutes after ATP application in the Ca^{2+} -containing bathing solution was 30 ± 6 of that in Ca^{2+} free solution (Fig. 4B). After a relatively long period following the ATP application (>20 minutes), an abrupt and very fast YO-PRO-1 and also lucifer yellow uptake was observed in some cells (14 ± 2 and 24 ± 8 of the cells for YO-PRO-1 and lucifer yellow uptake respectively) (Figs. 4A & 4B). This extracellular Ca^{2+} -dependent, delayed dye uptake component may indicate a delayed breakdown of the cell membrane induced by high levels of $[\text{Ca}^{2+}]_i$. The inhibitory effect of extracellular Ca^{2+} on uptake of anionic dye lucifer yellow can not be explained by a general inhibition of the P2X7 receptor responses caused by chelation of ATP^{4-} by the divalent cation, as the ATP-induced uptake of positively charged dye YO-PRO-1 remained clearly uninhibited.

In $[\text{Ca}^{2+}]_i$ measurements conducted with fura-2-loaded RAW 264.7 cells, we observed that, in Ca^{2+} (1 mM) containing bathing solution, ATP (1 mM) induced a large $[\text{Ca}^{2+}]_i$ increase compared to the nominally Ca^{2+} -free bathing solution (Fig. 5B inset. Average fura-2 fluorescence ratios observed 5 minutes after ATP application were 1.41 ± 0.08 and 0.58 ± 0.09 in the presence and absence of extracellular Ca^{2+} , respectively. $p < 0.01$). This result shows that in RAW 264.7 cells, changing the extracellular $[\text{Ca}^{2+}]$ from 0 to 1 mM, clearly augments the magnitude of the ATP-induced $[\text{Ca}^{2+}]_i$ increase, but is

ineffective on the uptake kinetics of YO-PRO-1. A summary of the ATP-induced dye uptake results in RAW 264.7 cells can be seen in Table 1.

Intracellular $[Ca^{2+}]_i$ Increase is not a Requirement for ATP-Induced YO-PRO-1 and Lucifer Yellow Uptake into RAW 264.7 Cells.

We incubated RAW 264.7 cells with BAPTA-AM (20 μ M for 60 minutes) and applied ATP (1 mM) in EGTA (1 mM)-containing nominally Ca^{2+} free bathing solution to buffer $[Ca^{2+}]_i$ increase and measured YO-PRO-1 and lucifer yellow uptake using a confocal microscope. This stringent buffering slowed or delayed, but did not abolish the ATP-induced YO-PRO-1 or lucifer yellow uptake (Figs. 5A and 5B). Slope of YO-PRO-1 uptake after ATP application in the Ca^{2+} -free bathing solution was $83 \pm 6\%$ of that in Ca^{2+} -containing solution. Lucifer yellow uptake started with an average delay of 2.05 ± 0.7 minutes in BAPTA-loaded cells compared to control cells. However once the uptake started, the rate of dye increase was similar to the control cells. (4 experiments performed as pairs on 4 days).

We used fura-2-loaded RAW 264.7 cells to control the effectiveness of our $[Ca^{2+}]_i$ buffering strategy. We observed no measurable $[Ca^{2+}]_i$ change after ATP application in any of the 3 experiments performed on 2 days, where both the intracellular and the extracellular $[Ca^{2+}]$ were buffered (Fig. 5B inset), indicating that the Ca^{2+} buffers we use can effectively prevent P2X7 receptor stimulated $[Ca^{2+}]_i$ increase in RAW 264.7 cells. These results show that an increase in $[Ca^{2+}]_i$ is not a prerequisite for ATP-induced permeabilization of RAW 264.7 cells to YO-PRO-1 or to lucifer yellow and uptake of both these dyes can occur even when $[Ca^{2+}]_i$ is rigorously buffered.

A Subpopulation of RAW 264.7 Cells Uptake Only Ethidium But Not Lucifer Yellow After ATP Stimulation. When lucifer yellow and ethidium were used simultaneously as tracers in confocal microscope measurements, we found that most of the RAW 264.7 cells took up both dyes, after ATP (1 mM) stimulation. This is an expected result as the

cells were shown to become permeable to both these dyes upon ATP stimulation in experiments performed separately. Unexpectedly, however, we observed that a subpopulation of cells which clearly took up ethidium did not show any sign of lucifer yellow entry. The rate of ethidium fluorescence increase in these cells was not different from those which readily took up both dyes (Fig. 6). The percentage of the cells that did not take up lucifer yellow was $23 \pm 6\%$ (4 experiments performed on 3 different days). This experiment reveals that activations of ethidium and lucifer yellow uptake through P2X7 receptor stimulation can occur independently on the same cell.

ATP-Induced Dye Uptake is Due to a Selective and Reversible Permeabilization

Process in Both HEK-rP2X7 and RAW 264.7 Cells. We limited the duration of all our dye uptake experiments to 20 minutes after the ATP application, in order to avoid cell-lysis which has been reported to occur in P2X7 receptor-expressing cells with longer ATP incubations (Pelegri and Surprenant, 2007). Nevertheless, to exclude the cell-lysis in our experiments, we checked if the ATP-induced cell membrane permeability could be reversed after the termination of the P2X7 receptor stimulation. Thus, we performed experiments where both the agonist and the dye were washed away after the 20-min-incubation with ATP and lucifer yellow (or calcein) and observed that the ratio of the dye-positive cells was significantly high compared to the control cells which were incubated without ATP (Supplement-Fig. 6). This finding indicates that in RAW 264.7 cells, inconsistent with a membrane breakdown, membrane permeability can quickly reverse and trap lucifer yellow or calcein inside the cytoplasm after termination of the ATP stimulation. We also observed that in HEK-rP2X7 cells, the ATP-induced permeability always retained a clear dye selectivity (Fig. 2). Furthermore, similar to the previously reported results (Pelegri and Surprenant, 2007), ATP-stimulated LDH release within 20 minutes was $4.1\% \pm 2\%$ of total cell LDH in our RAW 264.7 and

4.0% \pm 0.4% for HEK-rP2X7 cells. All of these results are inconsistent with a non-specific membrane breakdown and indicate a selective and reversible permeabilization process. Additionally, the apparent contrast between the homogenous distribution of lucifer yellow or calcein observed after ATP application and vesicular appearance of dye uptake observed in the absence of ATP clearly indicates that P2X7 receptor does not activate any pinocytotic mechanism (Fig. 1C).

Potential Experimental Artefacts. The methods employed to measure YO-PRO-1 and lucifer yellow uptakes are likely to have different detection efficiencies (YO-PRO-1 may be detected with a higher efficiency compared to lucifer yellow). In the hypothetical case where both HEK-rP2X7 and RAW cells have the same, non-selective dye permeability pathways, a smaller dye-conductance in HEK-rP2X7 cells, causing a slower lucifer yellow uptake, may keep the intracellular lucifer yellow dye below the detection limit. This in turn will give the wrong impression that these cells have a selective dye uptake mechanism for YO-PRO-1, which excludes lucifer yellow. According to this hypothesis, it should be expected that a smaller non-selective dye conductance results in an equally slower YO-PRO-1 uptake into HEK-rP2X7 cells compared to RAW cells. However our control experiments showed strictly the opposite: In the Ca-free solution, conductance of HEK-rP2X7 cells for YO-PRO-1 was drastically larger compared to RAW 264.7 cells (Supplement-Fig. 7). As we have already shown that lucifer yellow conductance is drastically smaller in HEK-rP2X7 cells (compare Fig. 2 with Fig. 4), we concluded that the P2X7-receptor stimulation does not activate a non selective permeation pathway on RAW and HEK cells, but it activates multiple pathways with different dye selectivities. These control experiments are explained in more detail in the legend of Supplement-Fig. 7.

Because anionic dye permeable pathway in HEK-rP2X7 cells is highly dependent on extracellular Ca^{2+} , it is plausible that calcein may have blocked its own ATP induced uptake by chelating and decreasing the extracellular free Ca^{2+} concentration. We controlled for this possible artefact by increasing extracellular $[\text{Ca}^{2+}]$ to 2 mM, thus avoiding the free concentration to fall below 1 mM. However we still observed no calcein uptake after ATP application under these conditions (Data not shown). We also confirmed that the Br-A23187 induced lucifer yellow increase in HEK-rP2X7 cells is due to an increase in intracellular $[\text{Ca}^{2+}]$ by showing that the ionophore has no effect in EGTA-containing bathing solution.

DISCUSSION

P2X7 receptor stimulation results in the activation of a permeability pathway on the cell membrane (Surprenant et al, 1996) which is generally believed to be formed by a non-selective pathway, probably a large pore-like structure that permeates all molecules with a molecular weight below ~1 KDa (North, 2002; Schilling et al, 1999; Steinberg et al, 1987). Other than its activation by P2X7 receptor, little is known about the identity and its permeation properties of the molecule (or molecules) that form this permeability pathway. In this study, we investigated the permeation and activation properties of the pathways that are responsible for the uptake of large fluorescent tracer molecules after P2X7 stimulation in HEK-rP2X7 and RAW 264.7 cells by using fluorescent dyes with different chemical structures, electrical charges and a wide range of molecular weights. Our results show that P2X7 receptor stimulation activates a complex array of permeation pathways that mediate uptake of fluorescent tracers into the cells. Our results can not be explained by the current idea of a single non-selective permeation pathway that is activated by P2X7 receptor. Instead, they suggest that at least two separate permeation pathways, with noticeably dissimilar selectivities and activation characteristics, are activated by P2X7 receptor.

In line with previous reports, we observed that application of extracellular ATP induced uptake of cationic fluorescent tracer molecules such as YO-PRO-1 (Fig. 2A) into HEK-rP2X7 cells (Surprenant et al, 1996; Virginio et al, 1999), cationic and also anionic tracers such as lucifer yellow (Fig. 4 and Supplement-Figs. 5 A and D) in to RAW 264.7 cells (Le Stunff and Raymond, 2007; Pelegrin and Surprenant, 2006; Steinberg, 1987). However, our observations revealed that the P2X7 receptor-activated dye-permeation processes are selective and stimulated in Ca^{2+} -free bathing solutions HEK-rP2X7 and RAW 264.7 cells present different selectivities. HEK-rP2X7 cells have

a permeability that is selective for cationic dyes (Fig. 2, Supplement-Fig. 2) whereas RAW 264.7 cells have a non-selective permeability (Fig. 4, Supplement-Figs. 5). This cationic dye pathway permeable to YO-PRO-1- on HEK-rP2X7 cells appears to be Ca^{2+} -independent as stringent buffering of $[\text{Ca}^{2+}]_i$ does not seem to block its activation (Fig. 3B). However there is an additional P2X7 receptor-activated dye uptake pathway on HEK-rP2X7 cells, which is permeable to anionic dye lucifer yellow and can not be activated in Ca^{2+} -free bathing solutions (Fig. 2B). This Ca^{2+} -dependent and lucifer yellow-permeable pathway appears to be very selective and does not permeate the anionic dye calcein (Fig. 2C). Additionally, it does not seem to be permeable to YO-PRO-1 and TO-TO-1, as extracellular Ca^{2+} does not increase uptake rate of these dyes (Figs. 2A, 3A and also Supplement-Fig. 2). Also in HEK-rP2X7 cells increasing intracellular Ca^{2+} with an ionophore, in the absence of P2X7 receptor activation, activates a lucifer yellow uptake without any measurable calcein or YO-PRO-1 permeability (Supplement Fig. 3). Suggesting that in HEK-rP2X7 cells the lucifer yellow-permeable uptake pathway can directly be activated by intracellular Ca^{2+} .

Furthermore, albeit many RAW 264.7 cells show a non-selective dye uptake our observation that a sub-population of RAW 264.7 cells uptake only ethidium but not lucifer yellow, while others can uptake both dyes after ATP stimulation (Fig. 6) suggests that the dye uptake process in RAW 264.7 cells, which is seemingly non-selective is actually composed of at least two different P2X7 receptor-activated permeation pathways; One is permeable to cationic ethidium, and the other to anionic lucifer yellow dye (alternatively the latter one can be non-selective). All these P2X7 receptor-activated pathways in RAW 264.7 cells are Ca^{2+} -independent as they can be activated under stringent Ca^{2+} -buffering (Fig. 5). A schematic representation of these dye uptake pathways in HEK-rP2X7 and RAW 264.7 cells is given in Fig. 7.

The pathways permeating the anionic dyes in RAW 264.7 and HEK-rP2X7 cells appear to be different; the one in HEK-rP2X7 cells is strictly Ca^{2+} -dependent and selective for lucifer yellow (i.e. do not permeate calcein) whereas the one in RAW 264.7 cells seem to be Ca^{2+} -independent and permeate both lucifer yellow and calcein. Interestingly, the lucifer yellow uptake in RAW 264.7 cells seems to be inhibited by extracellular Ca^{2+} to a certain extent (Fig. 4B). We do not know the exact mechanism behind this inhibition. However, as we did not observe any inhibitory effect of extracellular Ca^{2+} on the ATP-induced uptake of YO-PRO-1 (Fig. 4A) this inhibition is unlikely to be on the P2X7 receptor itself and may be on the permeation pathway.

In contrast to our results, Faria et al (2009), also by referring to previous works (Coutinho-Silva and Persechini, 1997; Faria et al, 2005), concluded that P2X7 receptor stimulation, as well as increasing intracellular Ca^{2+} by an ionophore, activate a non-selective pore with a large electrical conductance, which permeates both lucifer yellow and ethidium in HEK-293 cells. Additionally, pannexin-1, a gap-junction protein which forms a non-selective pore, has been shown to be involved in P2X7 receptor-induced dye permeability (Locovei et al, 2007; Pelegrin and Surprenant, 2006; Pelegrin and Surprenant, 2007). These results support the common view that a large non-selective permeabilisation pathway (an actual pore in these cases) is activated by P2X7 receptor. However in contrast to these studies, Schachter et al (2008) have concluded that ATP application stimulates a selective permeation pathway for negative dyes in P2X7 receptor-expressing HEK-293 cells and activates two permeation pathways; one non-selective, the other selective for negative dyes in macrophages. The study of Schachter et al (2008) and ours mutually confirm each other as independent studies using different experimental methods and indicate that P2X7 receptor activates selective solute-permeable pathways rather than a non-selective pathway or a “pore”. We used a more

quantitative method to measure the dye uptake, which allowed us to perform more vigorous control experiments.

The models which are represented schematically in Fig. 7 are the simplest models that can explain all our results. They show that at least two separate P2X7 receptor activated pathways, one mainly selective for cationic and the other mainly selective for anionic dyes, should exist in both HEK-rP2X7 and RAW 264.7 cells. The complexity of the real system may be higher than what is suggested in this scheme. For example, unlike our proposition, lucifer yellow and calcein may use two separate pathways to enter the RAW 264.7 cells. Instead of two selective pathways, one for anions and the other for cations, RAW 264.7 cells may have one non-selective and one cation-selective pathways. Additionally, it should be noted that instead of two separate proteins, a modification of the same protein (such as phosphorylation) may form these proposed pathways. It should also be stressed that the term “Ca²⁺-independent” which is used for some of the P2X7 receptor-activated dye permeation pathways observed in HEK-rP2X7 and RAW 264.7 cells, does not mean that these pathways can not be modulated by Ca²⁺.

The highly selective nature of the dye uptake pathway that we demonstrated may indicate that P2X7 receptor activates, instead of (or in addition to) a pore protein, a transporter or exchanger, similar to ABC transporters, which mediates the dye permeation. This hypothesis may help explaining not only the observations that suggest a selective dye permeation pathway but also all the puzzling findings showing that the dye permeable pathway, unexpectedly from a pore, does not contribute significantly to membrane currents; such as the findings that inhibition of pannexin-1 activity inhibits P2X7 receptor-induced dye uptake into HEK-293 and J774 cells without changing the membrane currents (Pelegriin and Surprenant, 2006), permeability to NMDG⁺ can be prevented without changing the YO-PRO-1 uptake (Jiang et al, 2005), or HEK-293 cells

remain impermeable to chloride ions while showing a clear YO-PRO-1 permeability after P2X7 receptor activation (Virginio et al, 1999).

In this study we presented evidence for the existence of at least two different and selective P2X7 receptor-activated permeation pathways in both HEK-rP2X7 and RAW 264.7 cells. We believe that the notion of P2X7 receptor-activated multiple permeation pathways with distinctly different selectivities, has an important bearing to the clarification of the physiological role of P2X7 receptor-induced permeabilization process in various cell types. Clearly, activation of a simple non-selective pore has implications for P2X7 receptor physiology that are completely different from those of a selective permeation mechanism. We believe that characterization of this mechanism is also important for a better understanding for utilization of P2X7 receptors for the delivery of large, membrane-impermeable drug molecules into cells and also devising uptake blockers for these pathways which (in contrast to receptor blockers) will interfere with only part of the P2X7 receptor-mediated signaling processes. Identification of the molecules forming these pathways and characterization of their selectivities for naturally occurring molecules remains to be clarified. We believe that our results will also be useful in the process of searching for candidate proteins that may be involved in P2X7 receptor-mediated permeabilization responses. We also present a new method for assessing the time course of the anionic fluorescent tracer uptake, for which, unlike DNA binding dyes, the fluorescence does not change significantly upon entering the cell. In combination with YO-PRO-1-like DNA-binding dyes, they form a valuable tool to identify the presence of different P2X7 receptor-activated permeation pathways not only in different cell types but in the same cell type as well.

ACKNOWLEDGEMENTS

We would like to thank Dr. Ozlem Ugur for her help in preparation of the stable HEK-293 clones and critically reading of the manuscript, Dr. Annemarie Surprenant (University of Manchester, Manchester, UK) for her gift of Cytotoxicity Detection Kit, Dr. Alan North (University of Manchester, Manchester, UK) for his generous gift of P2X7 receptor cDNA, Dr. Ongun Onaran and Dr. Nuhan Puralı (Hacettepe University, Ankara, Turkey) for a very helpful discussion. Part of this work was conducted in Ankara University Faculty of Medicine, Molecular Biology and Technology Research and Development Unit.

REFERENCES

- Bao L, Locovei S, Dahl G (2004) Pannexin membrane channels are mechanosensitive conduits for ATP. *FEBS Lett* **572**: 65-68
- Coutinho-Silva R, Persechini PM (1997) P2Z purinoceptor-associated pores induced by extracellular ATP in macrophages and J774 cells. *Am J Physiol Cell Physiol* **273**: C1793-1800
- Donnelly-Roberts DL, Jarvis MF (2007) Discovery of P2X7 receptor-selective antagonists offers new insights into P2X7 receptor function and indicates a role in chronic pain states. *Br J Pharmacol* **151**: 571-579
- Faria RX, De Farias FP, Alves LA (2005) Are second messengers crucial for opening the pore associated with P2X7 receptor? *Am J Physiol Cell Physiol* **288**: C260-271
- Faria RX, Reis RAM, Cascabulho CM, Alberto, A, de Farias FP, Henriques-Pons A, Alves LA (2009) Pharmacological properties of a pore induced by raising intracellular Ca²⁺. *Am J Physiol Cell Physiol* **297**: C28-42
- Jiang LH, Rassendren F, Mackenzie A, Zhang YH, Surprenant A, North RA (2005) N-methyl-D-glucamine and propidium dyes utilize different permeation pathways at rat P2X(7) receptors. *Am J Physiol Cell Physiol* **289**: C1295-1302
- Khakh BS, Bao XR, Labarca C, Lester H (1999) Neuronal P2X transmitter-gated cation channels change their ion selectivity in seconds. *Nature Neuroscience* **2**: 322-330
- Le Stunff H, Raymond MN (2007) P2X7 receptor-mediated phosphatidic acid production delays ATP-induced pore opening and cytolysis of RAW 264.7 macrophages. *Cell Signal* **19** : 1909-1918

- Locovei S, Bao L, Dahl G (2006) Pannexin 1 in erythrocytes: function without a gap. *PNAS* **103**: 7655-7659
- Locovei S, Scemes E, Qui F, Spray DC, Dahl G (2007) Pannexin1 is part of the pore forming unit of the P2X(7) receptor death complex. *FEBS Lett* **581**: 483-488
- North RA (2002) Molecular physiology of P2X receptors. *PhysiolRev* **82**: 1013–1067
- Pelegrin P, Surprenant A (2006) Pannexin-1 mediates large pore formation and interleukin-1beta release by the ATP-gated P2X7 receptor. *EMBO Journal* **25**: 5071-5082
- Pelegrin P, Surprenant A (2007) Pannexin-1 couples to maitotoxin- and nigericin-induced interleukin-1beta release through a dye uptake-independent pathway. *J Biol Chem* **282**: 2386–2394
- Ralevic V, Burnstock G (1998) Receptors for purines and pyrimidines. *Pharmacol Rev* **50**: 413–492
- Schachter J, Motta AP, de Souza Zamorano A, da Silva-Souza HA, Guimarães MZ, Persechini PM (2008) ATP-induced P2X7-associated uptake of large molecules involves distinct mechanisms for cations and anions in macrophages. *J Cell Sci* **121**: 3261-70
- Schilling WP, Wasylina T, Dubyak, GR, Humphreys BD, Sinkins WG (1999) Maitotoxin and P2Z/P2X(7) purinergic receptor stimulation activate a common cytolitic pore. *Am J Physiol Cell Physiol* **277**: C766-776
- Steinberg TH, Newman AS, Swanson JA, Silverstein SC (1987) ATP4- permeabilizes the plasma membrane of mouse macrophages to fluorescent dyes. *J Biol Chem* **262**: 8884–8888

Surprenant A, Rassendren F, Kawashima E, North RA, Buell G (1996) The cytolytic P2Z receptor for extracellular ATP identified as a P2X receptor (P2X7). *Science* **272**: 735–738

Virginio C, Church D, North RA, Surprenant A (1997) Effects of divalent cations, protons and calmidazolium at the rat P2X7 receptor. *Neuropharmacology* **36**: 1285–1294

Virginio C, MacKenzie A, North RA, Surprenant A (1999) Kinetics of cell lysis, dye uptake and permeability changes in cells expressing the rat P2X7 receptor. *J Physiol* **519**: 335–346

Yan Z, Li S, Liang Z, Tomić M, Stojilkovic SS (2008) The P2X7 receptor channel pore dilates under physiological ion conditions. *J Gen Physiol* **132**: 563-573

FOOTNOTES

*This work was supported by Ankara University research grant [BAP-2006 0809 232].

FIGURE LEGENDS

Fig. 1. P2X7 receptor stimulation causes shape change and uptake of anionic dyes

in HEK-rP2X7 and RAW 264.7 cells. HEK-rP2X7 and RAW 264.7 cells grown on cover slips were incubated with (**ATP 1**) or without (**ATP 0**) ATP (1 mM) for the indicated durations either in 1 mM Ca⁺²-containing (**Ca 1**) or nominally Ca⁺²-free (**Ca 0**) bathing solutions with lucifer yellow. Images were obtained with a confocal microscope. **A.** RAW 264.7 cells in the same field of view before (left panel) and 10 minutes after (middle panel) the application of 1 mM ATP, lucifer yellow uptake can clearly be seen after ATP application. No lucifer yellow uptake occurs in the control cells incubated in the same bathing solution for 20 minutes without ATP (right panel). **B.** No lucifer yellow uptake is visible in HEK-rP2X7 cells before (left panel) or 20 minutes after (middle panel) the application of 1 mM ATP in nominally Ca⁺² free bathing solution. However, lucifer yellow uptake is evident in cells incubated with 1 mM ATP for 10 minutes in 1 mM Ca⁺²-containing bathing solution (right panel). **C.** DIC (upper panels) and fluorescence images (lower panels) showing that RAW 264.7 cells can retain the dye after the wash out of ATP. Cells were incubated with ATP (1 mM) in nominally Ca⁺² free bathing solution for 20 minutes and then washed with a fresh bathing solution. (left panels). When cells were incubated in the same bathing solution without ATP for 20 minutes, the only observable dye uptake after wash out is vesicular (right panels). Images are 123 μ M (**A** and **B**) and 70 μ M (**C**) across.

Fig. 2. Presence of extracellular Ca⁺² alters the dye selectivity properties of the P2X7 receptor-activated permeability in HEK-rP2X7 cells. HEK-rP2X7 cells grown

on cover slips were stimulated with 1 mM ATP either in 1 mM Ca^{+2} containing (**ATP Ca 1**) or nominally Ca^{+2} free (**ATP Ca 0**) bathing solutions at the indicated time points. Control traces were obtained in Ca^{+2} -containing or nominally Ca^{+2} -free bathing solutions without ATP (**Control Ca 1** and **Control Ca 0** respectively). Time dependent uptake of YO-PRO-1 (**A**), lucifer yellow (**B**) or calcein (**C**) were observed as fluorescence increase within the cell by using a confocal microscope. All the results in **A, B and C** are representative for at least 3 independent experiments. In (**A**) total YO-PRO-1 fluorescence was measured from a cell population within a single field of view and initial fluorescence values were subtracted from each trace. In (**B**) and (**C**) traces show the ratio of intracellular average fluorescence to extracellular average fluorescence (**FIC/FEC**). Each trace is given as average \pm SEM of measurements from different cells in the same field of view. The experiments shown together in the same graph were performed on the same day with the same microscope settings.

Fig. 3. P2X7 receptor-stimulated YO-PRO-1 uptake in HEK-rP2X7 cells is independent from Ca^{+2} . YO-PRO-1 fluorescence increase was measured with a cuvette spectrofluorimeter and given as the ratio of measured fluorescence over maximum fluorescence obtained after Triton X-100 application (**F/Fmax**). 1 mM ATP was applied at the time point indicated by an arrow. Initial fluorescence values were subtracted from each trace. The experiments shown together in the same graph were performed on the same day. **A.** Suspended HEK-rP2X7 cells were stimulated either in 1 mM Ca^{+2} -containing (**ATP Ca 1**) or nominally Ca^{+2} -free (**Ca 0**) solution. Each trace is the average \pm SEM of 6 independent experiments performed as pairs. **B.** BAPTA-loaded HEK-rP2X7 cells were suspended in EGTA (1 mM)-containing Ca^{+2} -free (**ATP BAPTA-EGTA**) or unloaded cells were suspended in nominally Ca^{+2} -free (**ATP Ca 0**)

bathing solution. Traces are average \pm SEM of 5 independent experiments performed as pairs. **Inset for B.** $[Ca^{2+}]_i$ measurement after ATP (1 mM) application in suspended HEK-rP2X7 cells given as fluorescence ratio of Fura-2 signal (**F340/F380**).

Measurements were performed in the same bathing solutions and with BAPTA loaded or unloaded cells as in (**B**). Traces are representative of 3 independent experiments.

Fig. 4. ATP stimulation activates YO-PRO-1 and lucifer yellow uptake into RAW 264.7 cells . RAW 264.7 cells grown on cover slips were stimulated with 1 mM ATP in either Ca^{+2} (1 mM)-containing (**ATP Ca 1**) or nominally Ca^{+2} -free bathing solutions (**ATP Ca 0**). **A.** YO-PRO-1 uptake was measured as described in figure 2 but each trace shows the average \pm SEM of time dependent change in fluorescence signals measured from individual cells within a single field of view. Note that, in Ca^{+2} -containing solution, the early phase of the YO-PRO-1 uptake is unchanged but a second uptake component appears after a delay. **B.** Lucifer yellow uptake was measured and presented as described in **Figure 2**. Note that the early phase of lucifer yellow uptake is abolished but another component appears after a delay period in Ca^{+2} -containing solution.

Fig. 5. P2X7 receptor-stimulated YO-PRO-1 and lucifer yellow uptake in RAW 264.7 cells do not show any clear dependence on Ca^{+2} . ATP (1 mM)-induced YO-PRO-1 (**A**) or lucifer yellow (**B**) uptake by RAW 264.7 cells were measured in either BAPTA-loaded cells in Ca^{+2} -free bathing solution that contains 1 mM EGTA (**ATP BAPTA-EGTA**) or unloaded cells in nominally Ca^{+2} -free bathing solution (**ATP Ca 0**). YO-PRO-1 and lucifer yellow uptakes were measured and presented as described in figure 4 and figure 2 respectively. The experiments shown together in the same graph were performed on the same day with the same microscope settings. **Inset for B.** $[Ca^{2+}]_i$

increase in RAW 264.7 cells after 1 mM ATP application. Bathing solutions used in these measurements were the same as in **(B)**, except for the 1 mM Ca^{2+} containing solution (**ATP Ca 1**). Results are given as fluorescence ratio of fura-2 signal (**F340/F380**). Traces are representative of 4 independent experiments.

Fig. 6. P2X7 receptor stimulation activates two permeability responses with different selectivities in RAW 264.7 cells.

RAW 264.7 cells grown on cover slips were stimulated with 1 mM ATP in nominally Ca^{+2} -free bathing solution. Lucifer yellow and ethidium uptake by RAW 264.7 cells were recorded simultaneously. **A.** Confocal images taken just before (**ATP 1, 0 minutes**) and 20 minutes after ATP (1 mM) application (**ATP 1, 20 minutes**), showing lucifer yellow (upper panel) and ethidium (lower panel) fluorescence. Two types of cell response are noticeable; while all cells uptake ethidium, only some uptake lucifer yellow. **B.** ATP-induced lucifer yellow (upper panel) and ethidium uptakes (lower panel) measured from two different RAW 264.7 cells that are marked in the confocal images in panel **A** as **Cell 1** and **Cell 2** which represent two different types of dye uptake response. **Cell 1** uptakes both lucifer yellow and ethidium, **Cell 2** uptakes only ethidium, but not lucifer yellow. In ethidium uptake measurements, initial fluorescence values were subtracted from the traces to facilitate comparison. Images are 123 μM across.

Fig. 7. Schematic representation of two distinct dye uptake pathways proposed to be present in HEK-rP2X7 and RAW 264.7 cells. One of them is permeable to cationic and the other to anionic dyes. In HEK-rP2X7 cells, P2X7 receptor (**P2X7-R**) stimulation seems to activate at least two distinct and selective dye uptake pathways.

One of them is permeable only to lucifer yellow (but not to YO-PRO-1) and its activation seems to be mediated by an increase in the $[Ca^{2+}]_i$. The other pathway is independent from Ca^{2+} and permeable to YO-PRO-1 but not to lucifer yellow. In RAW 264.7 cells, P2X7 receptor activates again two distinct pathways. One is permeable to lucifer yellow, and the other to ethidium (but not to lucifer yellow). Neither of them show a clear Ca^{2+} dependence for activation. The anionic dye-permeable pathway in HEK-rP2X7 cells seems to differ from the one in RAW 264.7 cells in that it is Ca^{2+} independent and impermeable to calcein.

TABLES

	HEK-rP2X7				RAW 264.7			
	Lucifer yellow	Calcein	YO-PRO-1	TO-TO-1	Lucifer yellow	Calcein	YO-PRO-1	TO-TO-1
Ca 0	-	-	+	+	+	+	+	+
Ca 1	+	-	+	+	Slowed	Slowed	+	+
A23187	+	-	-					

Table 1. Effect of extracellular Ca⁺² on P2X7 receptor-activated uptake of different dyes in HEK-rP2X7 and RAW 264.7 cells. ATP (1 mM) is applied either in nominally Ca⁺²-free (**Ca 0**) or in 1 mM Ca⁺²-containing (**Ca 1**) bathing solution to HEK-rP2X7 and RAW 264.7 cells. Br-A23187 (10 μM) is applied in 5 mM Ca⁺²-containing (**A23187**) bathing solution to HEK-rP2X7 cells. Plus sign indicates the presence and minus sign the absence of uptake of the specified dye into the specified cell type. “Slowed” indicates that the uptake rate of the specified dye is measurably decreased by the presence of Ca⁺² in the bathing solution.

Figure 1

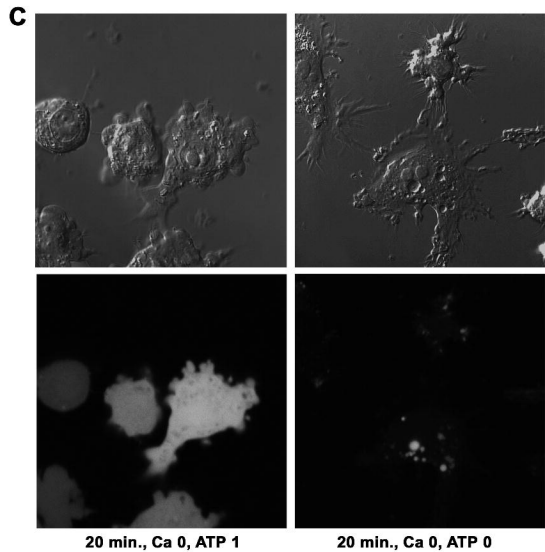
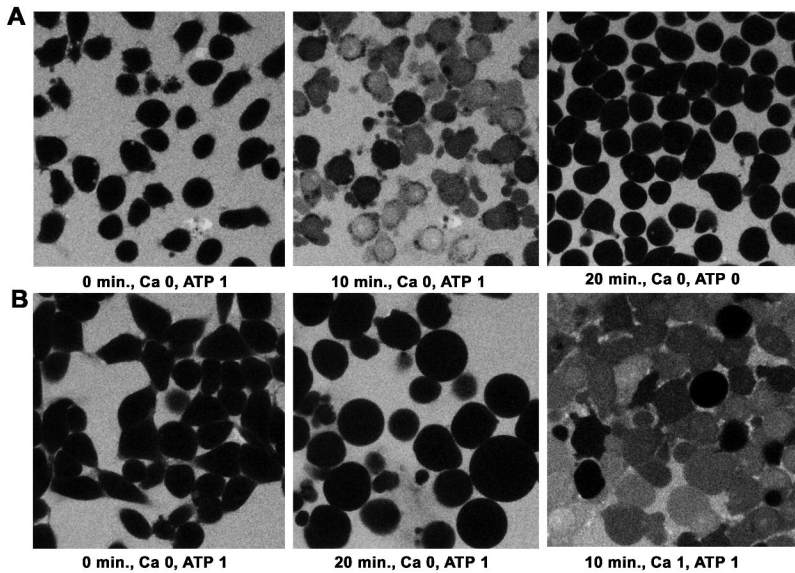


Figure 2

org at ASPET Journals on April 19, 2024

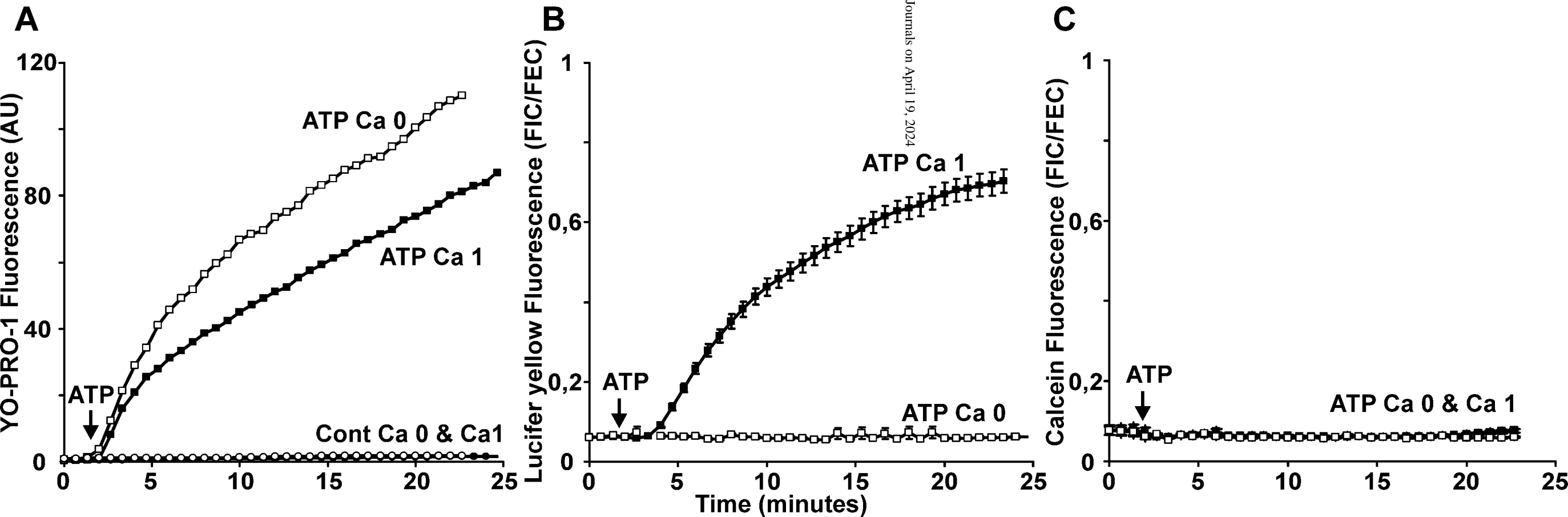


Figure 3

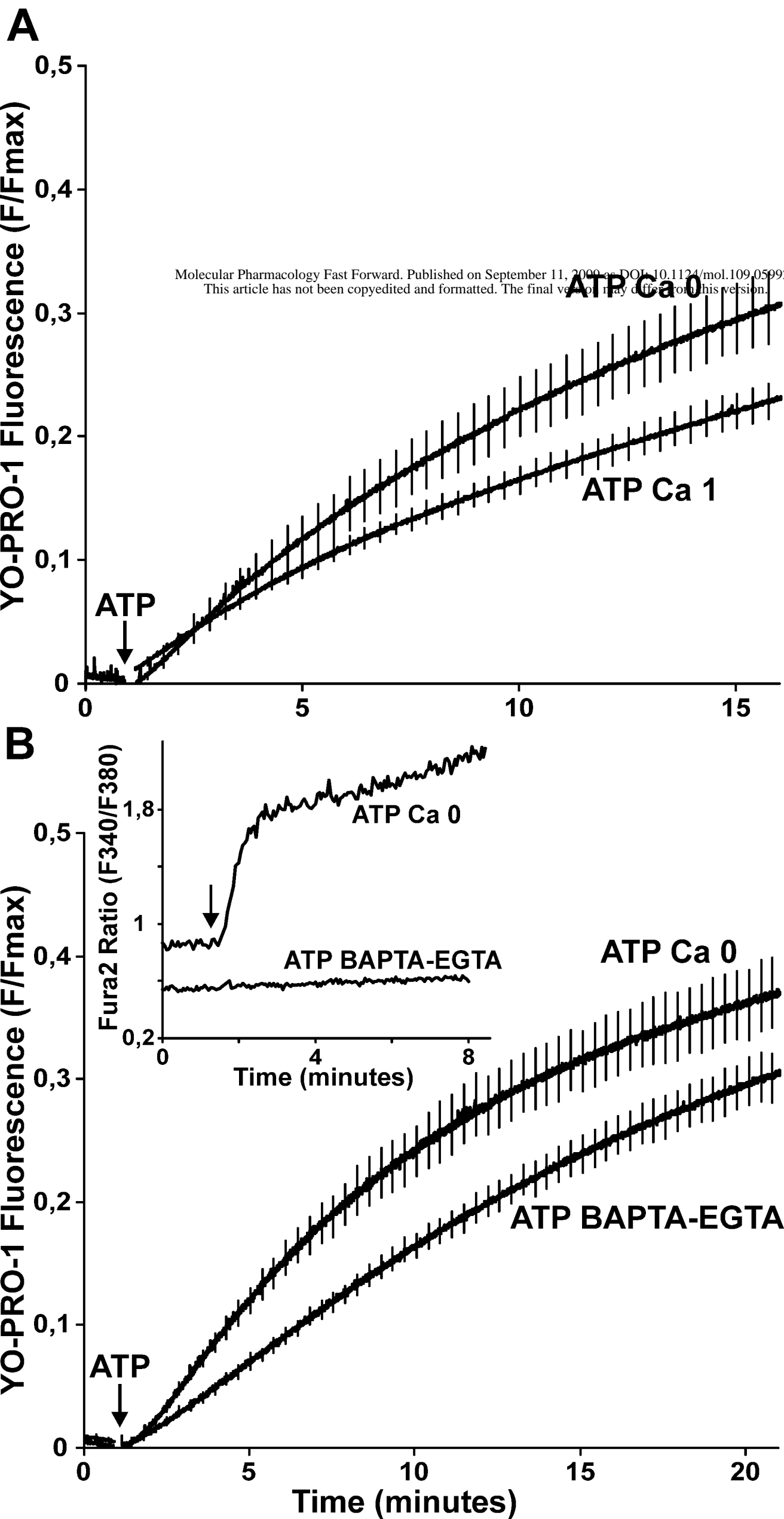


Figure 4

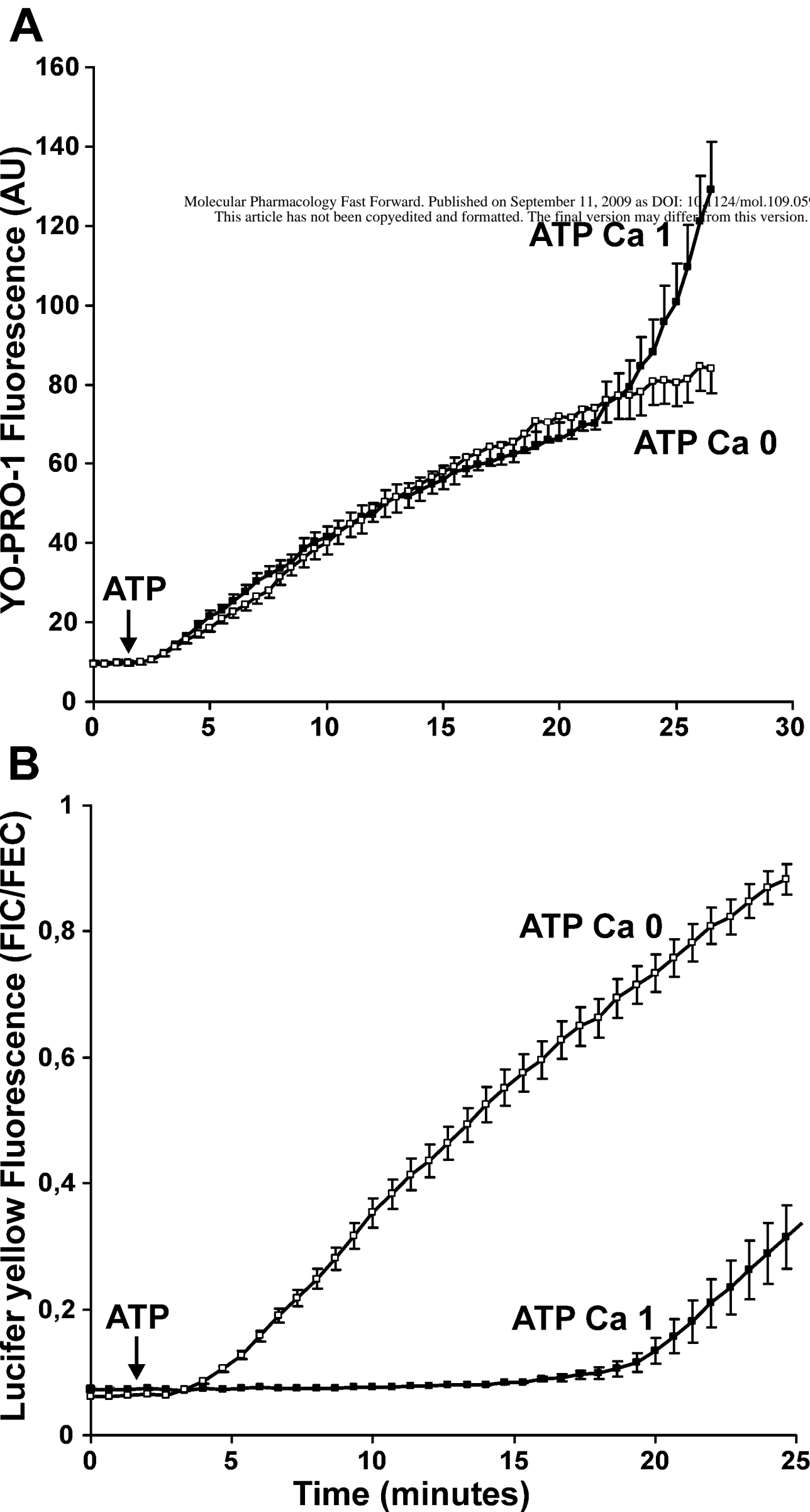


Figure 5

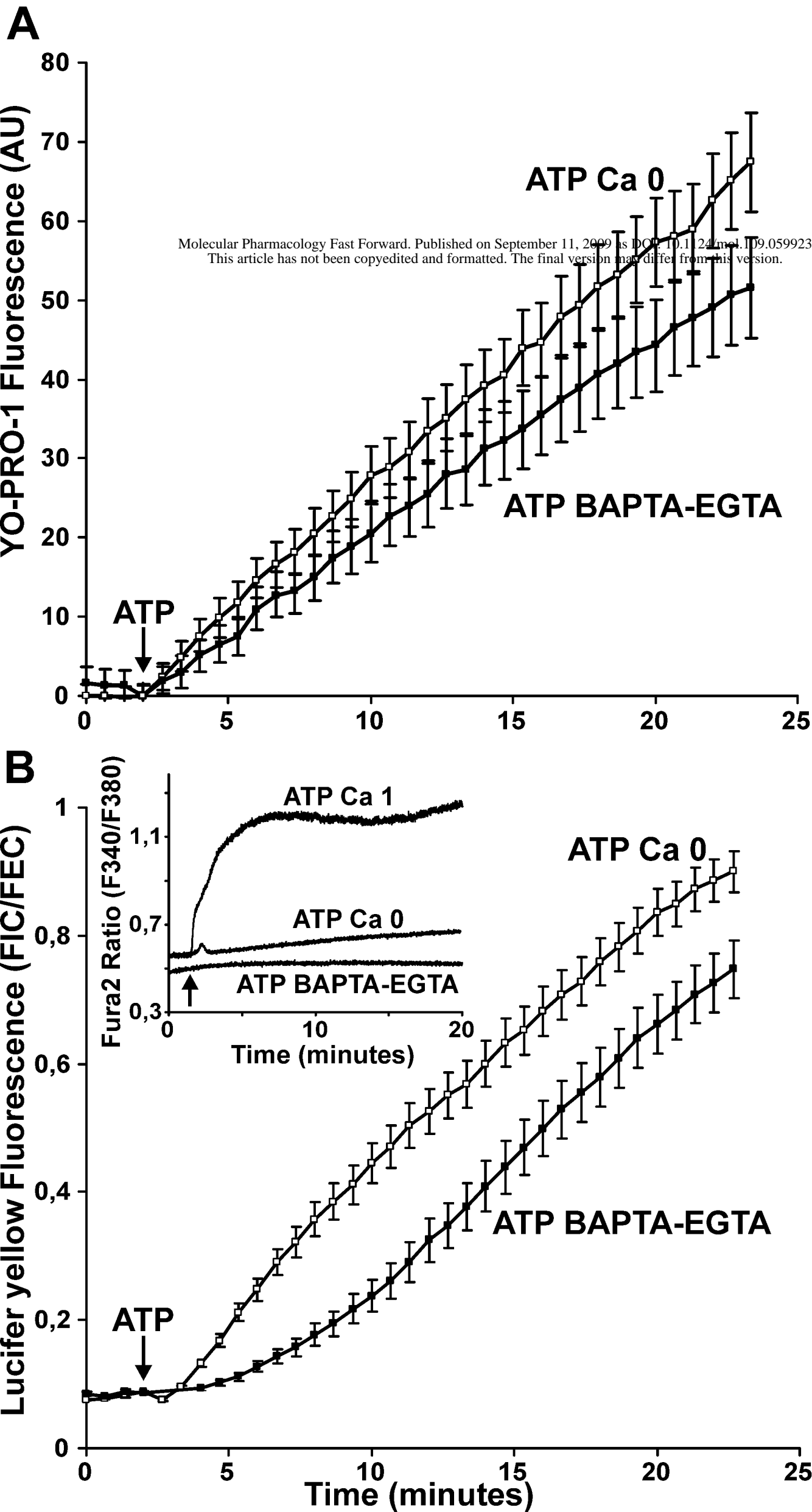


Figure 6

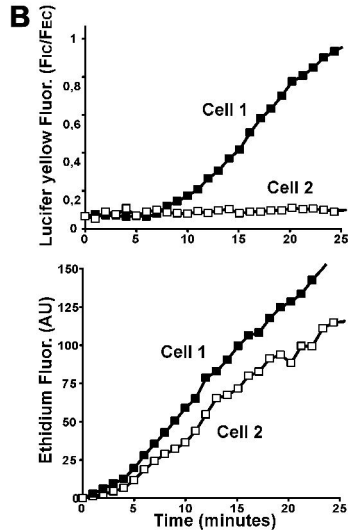
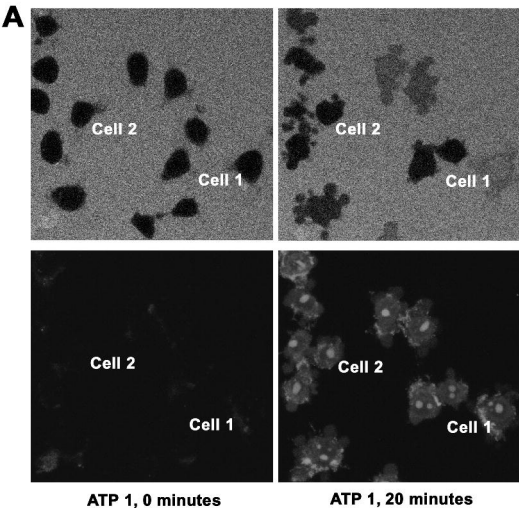


Figure 7

